How to cite: *Angew. Chem. Int. Ed.* **2023,** *62,* e202218907
International Edition: doi.org/10.1002/anie.202218907
German Edition: doi.org/10.1002/ange.202218907

Lewis Acids

A Bidentate Ligand Featuring Ditopic Lewis Acids in the Second Sphere for Selective Substrate Capture and Activation

*Daniel M. Beagan, John J. Kiernicki, Matthias Zeller, and Nathaniel K. Szymczak**

Abstract: We present a ligand platform featuring appended ditopic Lewis acids to facilitate capture/activation of diatomic substrates. We show that incorporation of two 9-borabicyclo[3.3.1]nonane (9-BBN) units on a single carbon tethered to a pyridine pyrazole scaffold maintains a set of unquenched nitrogen donors available to coordinate Fe^{II}, Zn^{II}, and Ni^{II}. Using hydride ion affinity and competition experiments, we establish an additive effect for ditopic secondary sphere boranes, compared to the monotopic analogue. These effects are exploited to achieve high selectivity for binding NO_2^- in the presence of competitive anions such as F^- and NO_3^-. Finally, we demonstrate hydrazine capture within the second-sphere of metal complexes, followed by unique activation pathways to generate hydrazido and diazene ligands on Zn and Fe, respectively.

To capture and reduce biologically relevant substrates with high specificity, the active site(s) of metalloenzymes often feature surrounding secondary sphere groups that accommodate multiple points of binding (multitopic hydrogen bond donors/acceptors).[1] These units facilitate selective substrate binding with high affinity at sites that might otherwise bind with low affinity. Substrate binding/recognition serves as the key first step to dictate structure, function, and product distribution.[2] One strategy to emulate these design principles within a synthetic system is to couple a Lewis acidic group with a metal site via a covalently linked tether.[3] While H-bonds are routinely used within enzyme active sites, Lewis acids provide a complementary approach because of their steric/electronic versatility and their stability to highly reducing environments.[4] This approach has facilitated C–C bond coupling of CO ligands,[5] ligand exchange,[6] oxidative addition,[7] and hydride transfer.[8] However few systems contain secondary sphere groups that mimic di/poly-topic units.[3] To distinguish this work from reported ligand scaffolds containing multiple second-sphere boranes, we define ditopic boranes as a *pre-organized* unit with two boranes predisposed for multi-point binding of substrates. Our group has previously investigated cooperative binding modes and subsequent reactivity enabled by Lewis acidic borane-appended ligands.[4,9] To complement these efforts and parallel bifurcated H-bonds, we targeted a ditopic borane Lewis acid analogue amenable to incorporation within a ligand platform to ultimately facilitate cooperative substrate binding/activation.

1,1-diborylalkane units (Figure 1) have been previously used for a range of electrophilic couplings, nucleophilic additions, and catalytic borylation of arenes.[10] Preorganized ditopic boranes enable CO_2 activation in the presence of $^tBu_3P$,[11] and $1e^-$ and $2e^-$ trapping.[12] Ditopic boranes of linkages $B(C_n)B$ $(n>1)$ have been exploited for anion recognition,[13] hydrazine and dinitrogen capture,[14] olefin polymerization cocatalysts,[15a-e] and inverse electron-demand Diels-Alder catalysts.[15f] Despite the versatility of ditopic

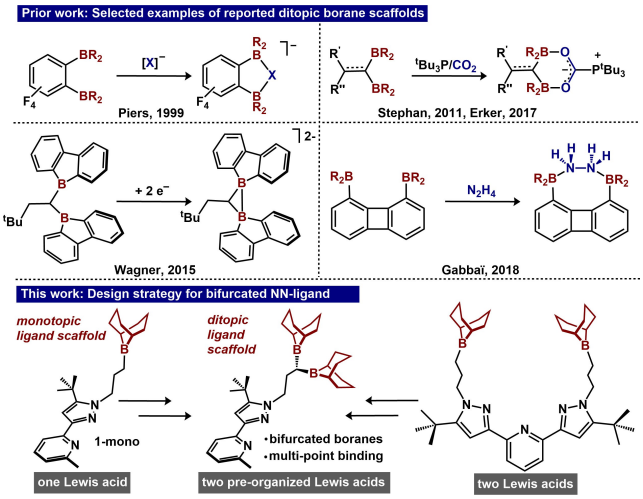

Figure 1. Selected examples of known ditopic boranes,[11,12b,14,15e] and design strategy outlining the ditopic ligand used in this work from prior work using a bidentate ligand with single second-sphere Lewis acid,[9a–c] and a tridentate ligand with two Lewis acids.[4,9d,e]

[*] Dr. D. M. Beagan, Dr. J. J. Kiernicki, Prof. N. K. Szymczak
Department of Chemistry, University of Michigan
930 N. University, Ann Arbor, MI 48109 (USA)
E-mail: nszym@umich.edu
Dr. M. Zeller
H.C. Brown Laboratory, Department of Chemistry, Purdue University
560 Oval Dr., West Lafayette, IN 47907 (USA)
Dr. J. J. Kiernicki
Present address: Drury University, Department of Chemistry and Physics
900 North Benton Ave., Springfield, MO 65802 (USA)

boranes, their extension to cooperative substrate binding/functionalization is under-explored, and they have not been incorporated into a ligand scaffold for this purpose. Herein, we report the synthesis of a ligand platform containing bifurcated second-sphere Lewis acids, evaluate the additive Lewis acidity and selective substrate binding, and describe their associated metal complexes as well as subsequent reactivity toward small molecules.

We targeted the diborane-appended pyridine pyrazole ligand through alkyne double hydroboration. The key synthon, a progaryl-appended ligand ($^{propargyl}NN^{tBu}$) was prepared in one step using a modification of a route previously used by our group for a related single borane Lewis acid.[9b] Addition of two equivalents of 9-borabicyclo-[3.3.1]nonane (9-BBN) to $^{propargyl}NN^{tBu}$ at 55 °C in C_6H_6 solvent resulted in the double anti-Markovnikov hydroboration product to afford ($^{(BBN)2}NN^{tBu}$) (**1**). Despite the presence of Lewis basic pyridine and pyrazole groups, both boranes were unquenched, as assessed by a broad resonance at 89.3 ppm in the ^{11}B NMR spectrum. This result contrasts with the monoborylated variant (**1-mono**) which features a quenched (intramolecular Lewis acid/base interaction) borane ($^{11}B = 39.2$ ppm): a difference we attribute to an increased steric profile of the Lewis acids. We found that the outcome of the hydroboration reaction was influenced by whether the ligand was first metalated. When ($^{propargyl}NN^{tBu}$) was combined with MBr_2 (M = Fe or Zn), forming ($^{(propargyl)}$-NN^{tBu})MBr_2 (Figure 2a), and then treated with 2 equivalents 9-BBN, the alkyne underwent a *single* hydroboration as established by single crystal X-ray diffraction (XRD) (M = Fe) and ^1H NMR spectroscopy (M = Zn, Fe) to generate the hydroborated alkene complexes ($^{(ene)}NN^{tBu}$)MBr_2 (Figure 2).[16]

To assess the competency of **1** to engage in bidentate binding to metal centers, we targeted metalation of Fe, Ni and Zn. Metalation of **1** with $FeBr_2$, (DME)$NiBr_2$, or ZnX_2 (X = Cl, Br) in THF solvent afforded the respective divalent metal complexes in high yields (Figure 2a). Complex ($^{(BBN)}$-$^2NN^{tBu}$)$FeBr_2$ (**2**) is high-spin ($\mu_B = 5.4$, THF, 22 °C) and displays solution C_s symmetry with ^1H NMR resonances between −27 and +53 ppm. **2** exhibits a reversible reduction wave in the cyclic voltammogram at −2.23 V (vs. Fc/Fc^+; 0.1 M $[Bu_4N][PF_6]$ in THF). This potential is cathodically shifted by 110 mV compared to singly borylated ($^{(BBN)}$-NN^{tBu})$FeBr_2$, consistent with modest electronic differences between the two ligands. Complex ($^{(BBN)2}NN^{tBu}$)$NiBr_2$ (**3**) is high-spin ($\mu_B = 2.9$, THF, 22 °C), and replacement of Fe with Ni results in an 880 mV anodic shift of the M^{II}/M^{I} redox couple. Finally, we prepared the Zn complexes ($^{(BBN)}$-$^2NN^{tBu}$)ZnX_2 (**4-X; X = Br, Cl**) to examine the system in the absence of a redox-active metal. The molecular structures of complexes **2–4** were established using single crystal XRD. Each isostructural complex displays tetrahedral geometry about the metal center ($\tau_4 = 0.84$–0.89), and the secondary sphere diboranes are geometrically unperturbed after metalation. The bifurcated Lewis acids exhibit average B–B bond distances of 2.486 Å, with an average ΣB = 359.41°, indicative of unquenched, trigonal planar boranes.

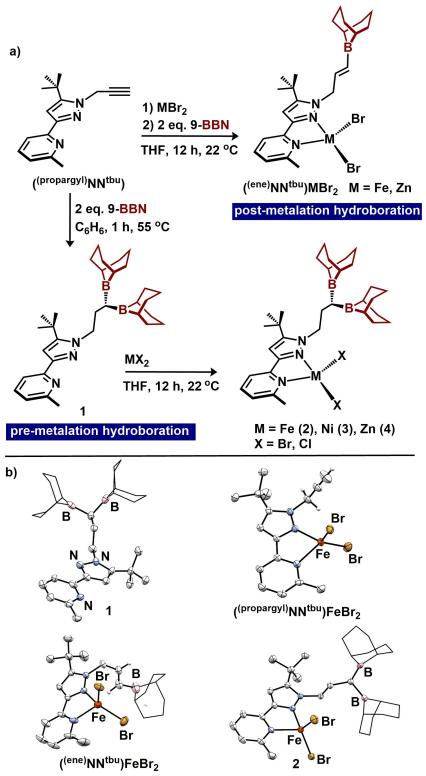

Figure 2. a) Synthesis of $^{(ene)}BBN^{tBu}FeBr_2$ via post-metalation hydroboration and synthesis of **1** and **2–4** via pre-metalation hydroboration b) molecular structures (50% probability ellipsoids) of **1**, ($^{(propargyl)}$-BBN^{tBu})$FeBr_2$, ($^{(ene)}BBN^{tBu}$)$FeBr_2$, and **2**. H-atoms excluding (ene) and (propargyl) groups are omitted, and the 9-BBN substituents are displayed in wireframe for improved clarity.

To assess the ability of **1** to serve as a ditopic acid and exert a Lewis acid additive effect compared to **1-mono** (Figure 1), we evaluated its Lewis acidity and substrate binding properties. Although Brønsted acidity is routinely assessed by pK_a values, Lewis acidity is substrate dependent, and defined against a reference Lewis base (e.g. F^-, $O{=}PEt_3$, H^-).[17] One of most commonly used methods to evaluate Lewis acidity is measurement of ^{31}P NMR chemical shifts of $O{=}PEt_3$/Lewis acid adducts that are transformed into an acceptor number (AN) (Gutmann-Beckett).[17a] We obtained opposing values when we used this method for a mono- and double-BBN containing ligand. Although **1-mono** provided an acceptor number (AN) of 23.8 (consistent with similar 9-BBN boranes),[9a] the AN of **1** was significantly lower and on par with that of solvent (5.9). Because a requirement of obtaining high ANs is formation of a strong acid/base adduct we attribute the low AN of **1** to the large steric profile of *both* –BBN groups, which we propose impedes $O{=}PEt_3$ adduct formation. To overcome these steric constraints, we assessed Lewis acidity using another commonly used method: fluoride ion affinity (FIA). The low steric profile of F^- allows binding in the bifurcated pocket of **1**; however, **1-mono** exhibited a larger FIA than **1** by 7.00 kcal mol^{-1}. We attribute the lower FIA of **1** to a geometric mismatch between the 1,1-diborylalkane empty p-orbitals and F^- lone pairs.

To assess Lewis acidity using a base with no orbital directionality, we calculated the hydride ion affinities (HIA) of **1** and **1-mono**. The size and spherical electron distribution of H^- mitigates both issues encountered using either the Guttman-Beckett method or FIA as metrical parameters for evaluating Lewis acidity. We found that the HIA of **1** is 15.7 kcal mol^{-1} greater than that of **1-mono**, implicating an additive effect exerted by the two second-sphere boranes (Figure 3c). For context, the 15.7 kcal mol^{-1} difference is similar to the hydride affinity difference between BH_3 and BEt_3.[18] Overall, these results underpin the complexity of Lewis acidity determination for gem-ditopic boranes, and suggest HIA is one of the few methods that allows direct Lewis acidity quantification across mono and ditopic acids.

Due to the high HIA of **1**, we targeted a 4-membered ring using hydride as a single atom bridge. Addition of 1 equiv KEt_3BH to **1** in THF generates a new species consistent with hydride adduct formation by ^{1}H and ^{11}B NMR spectroscopy.[19] The molecular structure of **1-H** (Figure 3a) confirms ditopic hydride capture. In the absence of 18-crown-6, the bidentate NN binding pocket sequesters the K^+ ion.

After assessing the Lewis acidity and HIA of **1**, we targeted adduct formation to evaluate the geometric preference of the ditopic diborane. We chose acetate as the ditopic Lewis base to first address the ability of **1** to form a 6-membered diboroheterocyle. Addition of KOAc to **1** in the presence of 1 equiv 18-crown-6 in THF solvent cleanly formed a new species (**1-OAc**), as indicated by ^{1}H and ^{11}B NMR spectroscopy. The molecular structure (Figure 3a) of **1-OAc** establishes κ^2-acetate capture, forming a 6-membered ring. We subsequently assessed binding with nitrite, which can coordinate either κ^2-N,O to form a 5-membered ring or κ^2-O,O to form a 6-membered ring. Upon addition of $NaNO_2$, nitrite binding to **1** occurs within 1 hour in THF at room temperature, and despite the oxophilicity of boron, the molecular structure of **1-NO$_2$** (Figure 3a) indicates a κ^2-N,O coordination mode of nitrite. The structurally characterized isomer was confirmed as the global minimum by density functional theory (DFT) (B3LYP-D3BJ/6-311 g-(d,p)) with κ^2-N,O coordination favored over κ^2-O,O by 4.7 kcal mol^{-1}.

Evaluation of the structural metrics of the 4-, 5-, and 6-membered diboroheterocycles (Figure 3b) indicates that the 2-atom bridge (nitrite) minimizes structural distortion of the ditopic unit when compared to **1**, exhibiting a slightly elongated B–B distance (+0.118 Å) and widening of the B–C–B angle (2.21°). The 6-membered ring in **1-OAc** affords B–B lengthening (+0.233 Å) and B–C–B angle widening (+8.4°) to a greater extent than **1-NO$_2$**. To accommodate a single atom bridge in **1-H**, the ditopic borane unit is significantly distorted compared to **1**, exemplifying B–B distance shortening (−0.561 Å) and considerable B–C–B angle contraction (−29.57°). To establish the extent to which the chelate effect of ditopic borane Lewis acid promoted adduct formation with ditopic Lewis bases, we used DFT to evaluate the thermodynamics for formation of both the acetate and nitrite adducts with 1 vs. 2 second-sphere boranes (Figure 3c). Notably, the formation of adducts with ditopic acids are more exergonic (compared

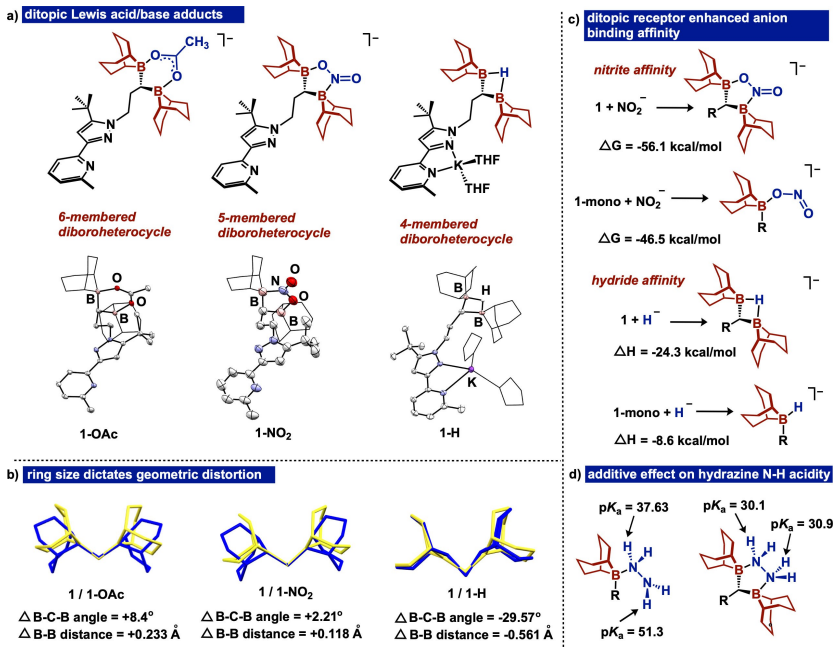

Figure 3. a) Anion capture mediated by **1** yielding ditopic boron containing heterocyles **1-OAc**, **1-NO$_2$**, and **1-H** and their respective molecular structures b) Comparison vs. free ligand (yellow) of distortion for ditopic borane unit with each heterocycle (blue) c) Comparative thermodynamics for nitrite and hydride capture for **1** and **1-mono** and d) Comparative pK_a values for hydrazine N–H protons. R represents the remainder of free ligand. Thermal ellipsoids displayed at 50% probability. H-atoms and counterions (in **1-OAc** and **1-NO$_2$**) are omitted, and the 9-BBN substituents and THF ligands in **1-H** are displayed in wireframe for improved clarity.

to monotopic counterparts) by 9.6 kcal mol^{-1} for nitrite and 12.1 kcal mol^{-1} for acetate.

To experimentally corroborate the 15.7 kcal mol^{-1} difference in HIA between **1** and **1-mono**, we executed both hydride competition and hydride transfer experiments. Addition of 1 equiv of KEt_3BH to a −78 °C THF solution containing 1 equiv of **1** and **1-mono** selectively generates **1-H** with unreacted **1-mono** by ^{1}H NMR spectroscopy. Further, addition of an isolated sample of monoborylated hydride **1-mono-H** to **1** in THF at 22 °C generates **1-H** and **1-mono**, substantiating the calculated HIA and implicating a low kinetic barrier for hydride transfer. To experimentally validate our hypothesis that pre-organized ditopic boranes can selectively coordinate ditopic Lewis bases through multi-point binding, we performed competition experiments with nitrite. Addition of 1 equiv $NaNO_2$ to a THF solution containing 18-crown-6 with 1 equiv of **1** and **1-mono** resulted in a color change to yellow, characteristic of **1-NO$_2$**. The ^{1}H NMR spectrum collected after 1 hour confirmed selective capture of NO_2^- by **1**, rather than **1-mono**. To assess the ability of the ditopic borane to selectively coordinate a dibasic substrate of higher Lewis basicity, we executed an analogous competition experiment with hydrazine (N_2H_4). Titration of N_2H_4 (two 0.5 equiv intervals) to a THF solution containing 1 equiv of both **1** and **1-mono** selectively generates **1-N$_2$H$_4$** (Figure 4) with **1-mono** unchanged as judged by ^{1}H NMR spectroscopy when integrated against a $(SiMe_3)_2O$ internal standard. To ensure that the self-quenching of **1-mono** was not affecting the competition experiment, we executed the same experiment with **4** and the monoborylated analogue **4-mono**. Similar to the free ligand, N_2H_4 selectively coordinates the ditopic receptor in **4**. The calculated DFT thermodynamics and competition experiments confirm a selective preference of ditopic Lewis bases to form chelates with the ditopic Lewis acids, compared to monotopic analogues.

To evaluate the extent to which **1** could be used for selective anion recognition, we performed an anion competition experiment. In contrast to *ortho*-phenylene and naphthalene based ditopic receptors, which have been reported as F^- sensors,[13] **1** exhibits a distinct selectivity preference for nitrite. Addition of a clear THF solution containing a mixture of 20 equiv F^-, 20 equiv NO_3^-, and 1 equiv NO_2^- (as $[NBu_4]^+$ salts) to a THF solution of **1** resulted in a color change to yellow. ^{1}H NMR spectroscopy confirmed a *single* product: **1-NO$_2$** (Figure 4).[20] This experiment indicates high NO_2^- affinity of **1**, even in the presence of anions that typically bind tightly to boranes, such as F^-. Overall, these results indicate that 1,1-diborylalkanes can be used as chemoselective molecular sensors for nitrite, which contrasts with the high F^- affinity of known ditopic borane receptors.

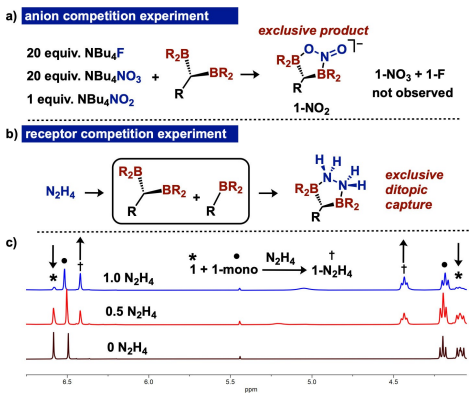

Figure 4. Anion competition reaction showing selective nitrite capture by **1** in the presence of fluoride and nitrate (top), selectivity of hydrazine binding to **1** in the presence of **1-mono** (middle) and ^{1}H NMR of hydrazine competition experiment (bottom) (N-C*H*$_2$ and pyz-C*H* shown). BR$_2$ = 9-BBN and R represents the remainder of the free ligand.

Upon establishing the viability of selective substrate capture using **1**, we examined the extent to which ditopic boranes could enable binding of reactive substrates adjacent to a metal site that would otherwise be unstable. Our group previously reported N_2H_4 Lewis acid/base adducts using Fe and Zn,[4a] and related work by the Gabbaï group showed $\mu_{1,2}$-hydrazine complexation using diboranes with large bite angles (B–B distances >4.5 Å).[14] Treating **2**–**4** with anhydrous N_2H_4 in THF proceeded smoothly to furnish the hydrazine adducts, **2-N$_2$H$_4$**, **3-N$_2$H$_4$**, and **4-N$_2$H$_4$**, respectively (Figure 5). The IR spectra contain two ν_{NH} bands between 3206 and 3296 cm^{-1}, and for **4-N$_2$H$_4$**, the ^{1}H NMR spectrum features a broad hydrazine N–H resonance at 6.44 ppm, while the ^{11}B NMR spectrum indicates equivalent tetrahedral boron atoms (1.3 ppm). The $\mu_{1,2}$ binding mode of hydrazine was unequivocally confirmed through SCXRD, with the molecular structures of the hydrazine adducts exhibiting isostructural second-sphere hydrazine coordination.

To further evaluate the additive effect of the ditopic boranes, we computed the pK_a values of the N–H protons of the hydrazine adduct **1-N$_2$H$_4$** (Figure 3d). The N–H protons of the hydrazine unit are more greatly acidified in **1-N$_2$H$_4$** (pK_a units = 30.9 and 30.1) compared to the monoborylated hydrazine adduct (pK_a units = 37.63 and 51.3). These data support an additive Lewis acidity effect for coordinated substrates to the ditopic borane unit, which complements prior reports for an additive effect through boron/zinc cooperativity.[9b]

After verifying the additive acidification of the N–H protons of chelated N_2H_4 adducts, we attempted selective deprotonation of ditopic borane hydrazine adducts. Addition of $KN(SiMe_3)_2$ to **1-N$_2$H$_4$** generates a mixture of products; however, deprotonation of metalated hydrazine adducts **2-N$_2$H$_4$** and **4-N$_2$H$_4$** afforded a distinct outcome. Dropwise addition of a freshly thawed $KN(SiMe_3)_2$ THF solution to a cold solution of **4-N$_2$H$_4$** afforded a white precipitate. The ^{1}H NMR and ^{11}B NMR spectra revealed reduced symmetry of the diborane tether, and the IR spectrum (KBr) exhibited ν_{NH} bands at 3292 and 3215 cm^{-1}, slightly shifted from **4-N$_2$H$_4$** (3288 and 3228 cm^{-1}). Two independent XRD experiments established connectivity and assignment of the hydrazido complexes ($^{(BBN)2}$NN^{tBu})ZnX(N_2H_3) (**5-X, X = Br, Cl**) (Figure 5), with the molecular structure of **5-Br** (Figure 5) showing retention of bifurcated acid/base binding

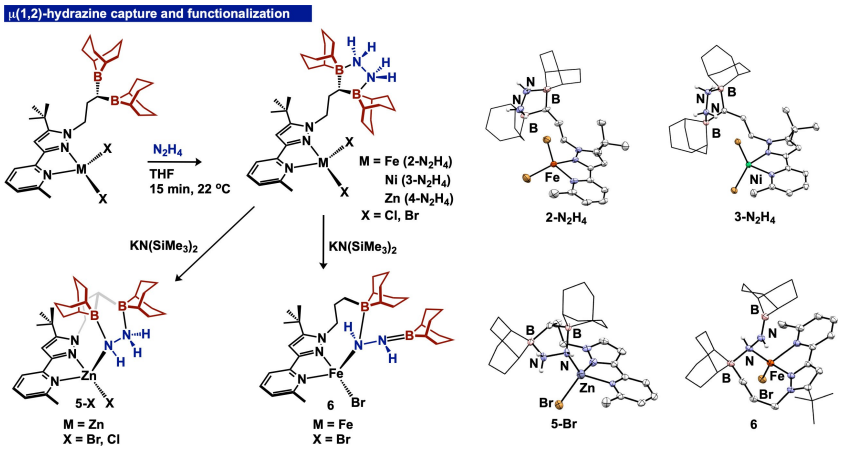

Figure 5. μ(1,2)-hydrazine capture using **2**–**4** to yield **2**–**4-N_2H_4** and hydrazine reactivity of **2-N_2H_4** and **4-N_2H_4** to generate hydrazido and diazene complexes **5-X** and **6** (X = Br, Cl). Molecular structures of **2-N_2H_4**, **3-N_2H_4**, **5-Br** and **6** (right). Thermal ellipsoids displayed at 50% probability. Non-diazene or hydrazine H-atoms are omitted, and the 9-BBN substituents are displayed in wireframe for improved clarity.

with the $N_2H_3^-$ ligand. We propose the difference in reaction outcomes between **1-N_2H_4** and **4-N_2H_4** is dictated by the placement of the generated highly reactive hydrazido unit, which in the latter case is directed toward the metal center, enabling cooperative stabilization by the metal and the ditopic second-sphere boranes. Complexes **5-Br** and **5-Cl** represent the first ditopic Lewis acid stabilized hydrazido ligands, an extension of prior work which stabilizes the Zn-N_2H_3 moiety through monotopic borane binding.[9a]

Replacement of Zn with Fe resulted in a distinct outcome. Addition of $KN(SiMe_3)_2$ to **2-N_2H_4** afforded a yellow compound whose solution structure (NMR) indicated reduced symmetry. The ν_{NH} bands in the IR spectrum appear at 3224, 3290 cm^{-1}, and are shifted from **2-N_2H_4** (3297, 3224 cm^{-1}). The molecular structure established through SCXRD revealed that the ligand underwent 9-BBN migration to cap the Fe-N_2H_2 diazene unit in **6** (Figure 5), with proton migration to the tether arm. The tethered 9-BBN interacts with the Fe coordinated α-N (B–N = 1.635 (3) Å), while the β-N is π-bound to the capped 9-BBN (B–N = 1.384(3) Å). The N–N distance (1.449(2) Å) is elongated compared to a similar π-delocalized Fe-N_2H_2 unit.[21] For electronic structure elucidation, we modelled **6** using DFT (See Supporting Information), and located the B–N π-bond in the HOMO-1. A comparison of the relative energies of isomeric **6** and the unobserved Fe-hydrazido complex indicate that **6** is more stable by 28.96 kcal mol^{-1}. The divergent product distribution for reactivity of **2-N_2H_4** and **4-N_2H_4** suggests that the incorporation of a redox-active metal unlocks mechanistic pathways for ligand rearrangement that are not viable with zinc.

In conclusion, we report the synthesis of a ligand with ditopic Lewis acids in the outer sphere. Metalation with iron, nickel, and zinc yields stable, tetrahedral complexes. The second-sphere mediates selective substrate capture including hydrazine, and functionalization of hydrazine leads to a hydrazido ligand on zinc and a diazene ligand on iron. An additive effect of the ditopic boranes was verified experimentally and computationally for substrate capture/activation. Given the appropriate substrate and synthetic conditions, **1** represents an attractive new class of ligands featuring bifurcated Lewis acids that can be exploited for small molecule activation.

Acknowledgements

This work was supported by the NIH (1R35GM13660-01). N. K. S. is a Camille Dreyfus Teacher-Scholar. X-ray diffraction equipment at Purdue University was supported by the National Science Foundation through the Major Research Instrumentation Program under Grant No. CHE 1625543. The authors thank Fengrui Qu for SCXRD data collection of **1**, **1-OAc**, **1-NO_2**, **1-H**, **2-Cl**, **3**, **3-N_2H_4**, **4**, **4-N_2H_4**, **5-Cl**, **5-Br**, and **6**.

Conflict of Interest

The authors declare no conflict of interest.

Data Availability Statement

The data that support the findings of this study are available in the supplementary material of this article.

Keywords: Chemoselective Anion Binding · Ditopic Boranes · Hydrazine Functionalization · Lewis Acids · Secondary Coordination Sphere

[1] a) A. S. Borovik, *Acc. Chem. Res.* **2005**, *38*, 54–61; b) T. Spatzal, K. A. Perez, O. Einsle, J. B. Howard, D. C. Rees, *Science* **2014**, *345*, 1620–1623; c) D. Sippel, M. Rohde, J. Netzer, C. Trncik, J. Gies, K. Grunau, I. Djurdjevic, L. Decamps, S. L. A. Andrade, O. Einsle, *Science* **2018**, *359*, 1484–1489; d) C. Van Stappen, Y. Deng, Y. Liu, H. Heidari, J.-

X. Wang, Y. Zhou, A. P. Ledray, Y. Lu, *Chem. Rev.* **2022**, *122*, 11974–12045; e) S. T. Stripp, B. R. Duffus, V. Fourmond, C. Léger, S. Leimkühler, S. Hirota, Y. Hu, A. Jasniewski, H. Ogata, M. W. Ribbe, *Chem. Rev.* **2022**, *122*, 11900–11973.

[2] a) P. C. Dos Santos, R. Y. Igarashi, H.-I. Lee, B. M. Hoffman, L. C. Seefeldt, D. R. Dean, *Acc. Chem. Res.* **2005**, *38*, 208–214; b) X. Zhang, K. N. Houk, *Acc. Chem. Res.* **2005**, *38*, 379–385; c) M. Prejanò, F. E. Medina, M. J. Ramos, N. Russo, P. A. Fernandes, T. Marino, *ACS Catal.* **2020**, *10*, 2872–2881; d) A. Warshel, P. K. Sharma, M. Kato, Y. Xiang, H. Liu, M. H. M. Olsson, *Chem. Rev.* **2006**, *106*, 3210–3235.

[3] M. W. Drover, *Chem. Soc. Rev.* **2022**, *51*, 1861–1880.

[4] a) J. J. Kiernicki, M. Zeller, N. K. Szymczak, *J. Am. Chem. Soc.* **2017**, *139*, 18194–18197; b) J. J. Kiernicki, J. P. Shanahan, M. Zeller, N. K. Szymczak, *Chem. Sci.* **2019**, *10*, 5539–5545.

[5] A. J. M. Miller, J. A. Labinger, J. E. Bercaw, *J. Am. Chem. Soc.* **2008**, *130*, 11874–11875.

[6] a) B. E. Cowie, D. J. H. Emslie, *Organometallics* **2015**, *34*, 2737–2746; b) B. E. Cowie, D. J. H. Emslie, *Can. J. Chem.* **2018**, *96*, 484–491.

[7] J. A. Zurakowski, B. J. H. Austen, M. C. Dufour, D. M. Spasyuk, D. J. Nelson, M. W. Drover, *Chem. Eur. J.* **2021**, *27*, 16021–16027.

[8] J. A. Zurakowski, M. Bhattacharyya, D. M. Spasyuk, M. W. Drover, *Inorg. Chem.* **2021**, *60*, 37–41.

[9] a) J. J. Kiernicki, E. E. Norwine, M. A. Lovasz, M. Zeller, N. K. Szymczak, *Chem. Commun.* **2020**, *56*, 13105–13108; b) J. J. Kiernicki, E. E. Norwine, M. Zeller, N. K. Szymczak, *Chem. Commun.* **2019**, *55*, 11896–11899; c) J. J. Kiernicki, E. E. Norwine, M. Zeller, N. K. Szymczak, *Inorg. Chem.* **2021**, *60*, 13806–13810; d) J. J. Kiernicki, M. Zeller, N. K. Szymczak, *Inorg. Chem.* **2019**, *58*, 1147–1154; e) J. J. Kiernicki, M. Zeller, N. K. Szymczak, *Inorg. Chem.* **2020**, *59*, 9279–9286; f) E. E. Norwine, J. J. Kiernicki, M. Zeller, N. K. Szymczak, *J. Am. Chem. Soc.* **2022**, *144*, 15038–15046; g) B. Wang, C. S. G. Seo, C. Zhang, J. Chu, N. K. Szymczak, *J. Am. Chem. Soc.* **2022**, *144*, 15793–15802.

[10] a) N. Miralles, R. J. Maza, E. Fernández, *Adv. Synth. Catal.* **2018**, *360*, 1306–1327; b) R. Nallagonda, K. Padala, A. Masarwa, *Org. Biomol. Chem.* **2018**, *16*, 1050–1064; c) Y-L. Liu, G. Kehr, C. G. Daniliuc, G. Erker, *Chem. Eur. J.* **2017**, *23*, 12141–12144.

[11] a) X. Zhao, D. W. Stephan, *Chem. Commun.* **2011**, *47*, 1833–1835; b) Y.-L. Liu, G. Kehr, C. G. Daniliuc, G. Erker, *Chem. Sci.* **2017**, *8*, 1097–1104.

[12] a) J. D. Hoefelmeyer, F. P. Gabbaï, *J. Am. Chem. Soc.* **2000**, *122*, 9054–9055; b) A. Hübner, T. Kaese, M. Diefenbach, B. Endeward, M. Bolte, H.-W. Lerner, M. C. Holthausen, M. Wagner, *J. Am. Chem. Soc.* **2015**, *137*, 3705–3714.

[13] a) C.-H. Chen, F. P. Gabbaï, *Angew. Chem. Int. Ed.* **2018**, *57*, 521–525; *Angew. Chem.* **2018**, *130*, 530–534; b) M. Melaïmi, S. Solé, C.-W. Chiu, H. Wang, F. P. Gabbaï, *Inorg. Chem.* **2006**, *45*, 8136–8143; c) S. Solé, F. P. Gabbaï, *Chem. Commun.* **2004**, 1284–1285.

[14] a) C.-H. Chen, F. P. Gabbaï, *Chem. Sci.* **2018**, *9*, 6210–6218; b) Z. Lu, H. Quanz, J. Ruhl, G. Albrecht, C. Logemann, D. Schlettwein, P. R. Schreiner, H. A. Wegner, *Angew. Chem. Int. Ed.* **2019**, *58*, 4259–4263; *Angew. Chem.* **2019**, *131*, 4303–4307; c) S. Xu, L. A. Essex, J. Q. Nguyen, P. Farias, J. W. Ziller, W. H. Harmann, W. J. Evans, *Dalton Trans.* **2021**, *50*, 15000–15002.

[15] a) J. Chai, S. P. Lewis, S. Collins, T. J. J. Sciarone, L. D. Henderson, P. A. Chase, G. J. Irvine, W. E. Piers, M. R. J. Elsegood, W. Clegg, *Organometallics* **2007**, *26*, 5667–5679; b) K. Köhler, W. E. Piers, A. P. Jarvis, S. Xin, Y. Feng, A. M. Bravakis, S. Collins, W. Clegg, G. P. A. Yap, T. B. Marder, *Organometallics* **1998**, *17*, 3557–3566; c) S. P. Lewis, L. D. Henderson, B. D. Chandler, M. Parvez, W. E. Piers, S. Collins, *J. Am. Chem. Soc.* **2005**, *127*, 46–47; d) S. P. Lewis, N. J. Taylor, W. E. Piers, S. Collins, *J. Am. Chem. Soc.* **2003**, *125*, 14686–14687; e) V. C. Williams, W. E. Piers, W. Clegg, M. R. J. Elsegood, S. Collins, T. B. Marder, *J. Am. Chem. Soc.* **1999**, *121*, 3244–3245; f) S. N. Kessler, H. A. Wegner, *Org. Lett.* **2010**, *12* (18), 4062–4065.

[16] See Supporting Information Pg S14 for more details of single vs. double hydroboration.

[17] a) M. A. Beckett, G. C. Strickland, J. R. Holland, K. Sukumar Varma, *Polymer* **1996**, *37*, 4629–4631; b) A. P. Lathem, Z. M. Heiden, *Dalton Trans.* **2017**, *46*, 5976–5985; c) L. O. Müller, D. Himmel, J. Stauffer, G. Steinfeld, J. Slattery, G. Santiso-Quiñones, V. Brecht, I. Krossing, *Angew. Chem. Int. Ed.* **2008**, *47*, 7659–7663; *Angew. Chem.* **2008**, *120*, 7772–7776; d) T. E. Mallouk, G. L. Rosenthal, G. Mueller, R. Brusasco, N. Bartlett, *Inorg. Chem.* **1984**, *23*, 3167–3173.

[18] M. T. Mock, R. G. Potter, D. M. Camaioni, J. Li, W. G. Dougherty, W. S. Kassel, B. Twamley, D. L. DuBois, *J. Am. Chem. Soc.* **2009**, *131*, 14454–14465.

[19] The ^{11}B NMR and ^{1}H NMR (hydride) signals observed are both broad singlets and show no B–H coupling, which is consistent with similar 9-BBN hydrides reported from our group (Refs. 9f and 4b).

[20] Free fluoride observed by ^{19}F spectroscopy (see Supporting Information for more details).

[21] C. T. Saouma, R. A. Kinney, B. M. Hoffman, J. C. Peters, *Angew. Chem. Int. Ed.* **2011**, *50*, 3446–3449; *Angew. Chem.* **2011**, *123*, 3508–3511.

[22] Deposition numbers 2214449, 2214450, 2214451, 2214452, 2214453, 2214454, 2214455, 2214456, 2214457, 2214458, 2214459, 2214460, 2214461, 2214462 and 2214463 contain the supplementary crystallographic data for this paper. These data are provided free of charge by the joint Cambridge Crystallographic Data Centre and Fachinformationszentrum Karlsruhe Access Structures service.

Manuscript received: December 21, 2022
Accepted manuscript online: January 31, 2023
Version of record online: February 20, 2023